ELSEVIER

Polymer 43 (2002) 1497–1502

polymer

www.elsevier.com/locate/polymer

A molecular dynamics study of the effects of branching characteristics of LDPE on its miscibility with HDPE☆

Zhengang J. Fan, Michael C. Williams, Phillip Choi*

Department of Chemical and Materials Engineering, University of Alberta, 536 Chemical & Materials Engineering Building, Edmonton, Alta., Canada T6G 2G6

Abstract

The effects of branching characteristics of low-density polyethylene (LDPE) on its melt miscibility with high-density polyethylene (HDPE) were studied using molecular simulation. In particular, molecular dynamics (MD) was applied to compute Hildebrand solubility parameters (δ) of models of HDPE and LDPE with different branch contents at five temperatures that are well above their melting temperatures. Values computed for δ agreed very well with experiment. The Flory–Huggins interaction parameters (χ) for blends of HDPE and different LDPE models were then calculated using the computed δ values. The level of branch content for LDPE above which the blends are immiscible and segregate in the melt was found to be around 30 branches/1000 long chain carbons at the chosen simulation temperatures. This value is significantly lower than that of butene-based linear low-density polyethylene (LLDPE) (40 branches/1000 carbons) in the blends with HDPE computed by one of the authors (polymer 2000; 41:8741). The major difference between LDPE and LLDPE models is that each modeled LDPE molecule has three long chains while each modeled LLDPE molecule had only one long chain. The present results together with those of the LLDPE/HDPE blends suggest that the long chain branching may have significant influence on the miscibility of polyethylene blends at elevated temperatures.

Keywords: Polyethylene blend; Molecular dynamics; Flory–Huggins interaction parameter

1. Introduction

The understanding of the phase behavior of polyethylene blends is of great commercial importance because in the polyethylene industry, different types of polyethylenes are often blended together to meet various kinds of requirements of processing and final products. In fact, various kinds of experimental techniques have been used to investigate the miscibility behavior of polyethylene blends and a great deal of information has been obtained from these efforts [1–15]. For example, it has been found that the branch content of linear low-density polyethylene (LLDPE) molecules is the controlling factor that determines the phase behavior of LLDPE/high-density polyethylene (HDPE) blends [1–6]. However, it terms of the cut-off value of the branch content for LLDPE in the blends with HDPE above which the components segregate and become immiscible, different views have been expressed in the literature [1,4,6,7]. In the cases of low-density polyethylene (LDPE)/HDPE and LDPE/LLDPE blends, there is also some basic disagreement about the general question of miscibility of blend components, some researchers reporting liquid–liquid phase separation [1,8–12,15], while others report complete melt homogeneity [4,13,14].

While a certain understanding of the miscibility of polyethylenes has been accumulated using the experimental techniques described in the above references, research on the same subject from either a theoretical or molecular modeling point of view has been scanty. The most recent attempt by Choi to model the blends of butene-based LLDPE and HDPE was one example [6]. In particular, he found that the branch content of LLDPE is the major factor determining the phase behavior of the butene-based LLDPE/HDPE blend. It was also predicted that the cut-off value for this blend is around 40 branches per thousand backbone carbons which is in good agreement with the findings of Alamo et al. [4] using the technique of small angle neutron scattering (SANS). Because of the successful match of the results obtained from molecular dynamics (MD) simulation with those of SANS, we are encouraged to use the same simulation approach to explore the miscibility

☆ This paper was originally submitted to *Computational and Theoretical Polymer Science* and received on 26 May 2001; accepted on 17 September 2001. Following the incorporation of *Computational and Theoretical Polymer Science* into *Polymer*, this paper was consequently accepted for publication in *Polymer*.

* Corresponding author. Tel.: +1-780-492-9018; fax: +1-780-492-2881.
E-mail address: phillip.choi@ualberta.ca (P. Choi).

0032-3861/02/$ - see front matter
PII: S0032-3861(01)00730-3

Table 1
Characteristics of the models used in the simulations

Model	Molar mass (g/mol)	Branch content[a], number of branches per 1000 long chain carbons
0	14,029	None
1	14,534	10
2	15,151	20
3	15,263	22
4	15,376	25
5	15,488	27
6	15,656	30
7	16,273	40

[a] Note: see text for the descriptions of the model number and the model shapes.

behavior of other polyethylene blends. In this paper, we report our recent results on the effects of temperature and branching characteristics of LDPE on its miscibility with HDPE.

2. Simulation methodology

In the simplest approach, miscibility is generally addressed in terms of the Hildebrand solubility parameters (δ) of the pure components comprising the blend. Determination of miscibility can be accomplished by calculating the Flory–Huggins interaction parameters (χ) for the binary mixtures of interest using the Hildebrand solubility parameter values of the pure polymers. In the present work, we adopted such a strategy by computing δ of both HDPE and LDPE with different branch contents based upon MD simulation and used such values to obtain χ and thus infer miscibility of each pair. The molecular simulation methodology we used is described in detail in Ref. [16]. In the following, this procedure will be described briefly.

Molecular simulations were carried out using a commercial software package, CERIUS2, version 3.5, developed by Molecular Simulations Inc., on a Silicon Graphics OCTANE workstation. Eight LDPE and HDPE molecular models were studied. The characteristics of the models are shown in Table 1 in which model 0 corresponds to HDPE (i.e. no branches); models 1–7 represent LDPE with different branch contents. The linear chain (HDPE model) consisted of 1000 carbons. Each LDPE molecule was modeled with three long chains and a certain number of short branches. The three long chains consisted of 500, 300 and 200 carbons.

Therefore, the total number of carbons contained in the three long chains for each LDPE model was 1000, thus matching the case for HDPE. The two long chains with 200 and 300 carbons were attached arbitrarily on the 86th carbon and the 350th carbon of the longest chains with 500 carbons. Short branches, containing four carbons, were randomly attached to various positions on the long chains. The branch contents for LDPE models were chosen with 10, 20, 22, 25, 27, 30 and 40 branches (including long and short branches) per 1000 long chain carbons. For example, the model with 10 branches here had four long chain ends and six short branches; the model with 20 branches had four long chain ends and 16 short branches. Note that most of the commercial LDPE products bear 15–30 branches/1000 carbons and among the branches, there may be one or two long branches. In this work, we have made every effort to construct representative models of the molecules in the LDPE commercial products. However, with the use of such a small molecule to represent LDPE, the number of long chain branches as well as their associated chain ends per unit volume of the material is inevitably high compared to those of the real polymer. Therefore, one should interpret the results with care. Other factors such as molecular weight distribution and variable chain lengths of short branches were not incorporated in our models due to the computational limitation. Once again, because of the size of the models, it was not practical to include hydrogen atoms explicitly in the simulations. As a result, a united atom approach was adopted [17].

The melt state of the molecular models was represented with the use of a cubic unit cell subject to periodic boundary conditions [17]. Each unit cell contained a single molecule and the size of the cell was constructed in such a way that its density matched with the available experimental value at a given temperature. The density values at the chosen simulation temperatures were determined based upon an empirical correlation developed by Rudin et al. [18]. The detailed procedures for constructing such initial structures are described in Refs. [6,16]. All initial structures created were energy-minimized using the conjugate gradient method before the MD simulations were begun.

Canonical (i.e. NVT) MD simulations were carried out at five different temperatures (425, 450, 475, 500 and 525 K) for all models based upon a scheme developed by Nosé [19] with a Leapfrog numerical algorithm [17]. By using the NVT ensemble, the densities can be controlled at the experimental values. Here, interested readers should refer to Ref. [6] for detailed discussion on the rationale for performing the simulations using NVT rather than NPT ensemble. For all models, simulation time was 1000 ps with a time step of 1 fs. All simulations showed that the total energy was leveling off within the last few hundred pico-seconds in the MD 'annealing', signifying that the systems had reached thermodynamic equilibrium. To check this, we repeated some of the calculations with different initial conformations for the same molecular models and found that they all reached approximately the same energy level, thus supporting our belief about the equilibrium nature of the results.

For the energy minimization and MD simulations, a generic force field, Dreiding 2.21, developed by Mayo et al. [20], was adopted because of its simplicity and the availability of united atom model parameters. The force field expressions and corresponding parameters are used to describe intra- and inter-molecular interaction energies

Table 2
Lennard-Jones parameters used for the simulations

United atom type	σ_0 (nm)	ε_0 (kJ/mol)
CH	0.3983	0.615
CH_2	0.4068	0.829
CH_3	0.4152	1.047

(E) that are assumed to have additive contributions from bonded (E_b) and non-bonded (E_{nb}) interactions

$$E = E_b + E_{nb} \quad (1)$$

where E_b includes bond stretching (E_s) that is described as a simple harmonic oscillator, bond angle bending (E_A) taken to be of the harmonic cosine form and torsion (E_T) described by more complex forms. Non-bonded interactions consist of van der Waals (E_{vdw}), electrostatic (E_Q), and explicit hydrogen bond (E_{hb}) terms. Thus, Eq. (1) can be written as:

$$E = E_S + E_A + E_T + E_{vdw} + E_Q + E_{hb} \quad (2)$$

Since polyethylenes are non-polar hydrocarbon polymers, E_Q is not significant and there is no E_{hb} involved. Therefore, E_{vdw} is the only non-bonded term being considered here. In Dreiding 2.21, E_{vdw} is described by a Lennard-Jones 12–6 potential. The corresponding Lennard-Jones parameters used here, estimated from crystal lattice spacing and heat of sublimation measurements for low molecular weight hydrocarbons, are shown in Table 2 [20]. Equilibrium carbon–carbon length and force constants used were 1.53 Å and 2930 kJ/mol/Å, respectively. Detailed descriptions of the Dreiding force field are given in Ref. [20].

Like many other classical force fields, Dreiding 2.21 often gives incorrect pressures when it is used with an NVT ensemble. For example, for the systems studied in the present work, the computed average pressures (Table 3) deviate significantly from the experimental value (1 atm or 0.1 MPa) at which the density was measured. Nevertheless, it is fortunate that Drieding 2.21 has been found to be capable of giving accurate estimates of δ values [6,16], especially for non-polar systems. Therefore, we feel that using such a generic force field is justified since the difference of solubility parameters of the two types of polyethylenes, $\Delta\delta$, is of major interest. However, it is not clear to us why Dreiding 2.21 can given accurate δ (see later) but not the pressure. This warrants further investigation.

3. Results and discussion

The Hildebrand solubility parameter, according to its definition, is calculated as follows:

$$\delta = [(E_{vac} - E_{cond})\rho/M]^{1/2} \quad (3)$$

Here, E_{vac} is the total energy of a mole of molecules in vacuum state while E_{cond} is the total energy in amorphous condensed state and the difference, $E_{vac} - E_{cond}$, is the cohesive energy of a mole of the melt. When this quantity is combined with the melt mass density ρ and molar mass M, $[(E_{vac} - E_{cond})\rho/M]$ becomes the well-known cohesive energy density. In this work, MD simulation was used to calculate both E_{vac} and E_{cond}.

Once the MD trajectories were created, the total energy values of each molecular model in vacuum and condensed states, computed for every 10 ps in the last 100 ps of the MD annealing, were averaged to obtain E_{vac} and E_{cond}, separately. In general, the standard deviations of the E_{vac} and E_{cond} values are less than 5% of their corresponding average values, indicating that such MD calculations are highly reproducible. Once both E_{vac} and E_{cond} were determined, individual solubility parameters were calculated for each model using Eq. (3). The detailed descriptions of the procedure are given in Ref. [16]. And the Flory–Huggins interaction parameter was thereby obtained.

$$\chi = (\delta_{HDPE} - \delta_{LDPE})^2 V/RT \quad (4)$$

Here, V is the molar volume of an ethylene unit at the simulation temperature T (i.e. the volume of a mole of lattice sites); R bears its usual meaning.

The computed Hildebrand solubility parameters of the polyethylene models are summarized in Table 4. In this table, the model code number bears the same meanings as in Table 1. The computed δ values agree very well with those obtained by Han et al. based upon pressure–volume–temperature (PVT) measurements [21]. For example, the experimental δ of HDPE at 166 °C is 17.8 ± 0.1 $MPa^{1/2}$ while the interpolated value of our computed δ of model

Table 3
Computed average pressures of the HDPE and LDPE models, (Mpa)

Model code	$T = 152$ °C	177 °C	202 °C	227 °C	252 °C
0	−196 ± 31	−154 ± 30	−136 ± 29	−128 ± 30	−121 ± 27
1	−83 ± 22	−81 ± 22	−81 ± 22	−74 ± 28	−70 ± 21
2	−76 ± 21	−77 ± 20	−71 ± 20	−75 ± 21	−62 ± 62
3	−37 ± 28	−78 ± 20	−73 ± 20	−65 ± 19	−63 ± 20
4	−78 ± 21	−84 ± 21	−83 ± 19	−71 ± 19	−59 ± 19
5	−79 ± 22	−80 ± 19	−68 ± 19	−68 ± 18	−69 ± 19
6	−79 ± 21	−84 ± 21	−74 ± 20	−74 ± 19	−70 ± 19
7	−87 ± 19	−72 ± 19	−66 ± 20	−64 ± 18	−61 ± 19

Table 4
δ, computed Hildebrand solubility parameters ($MPa^{1/2}$) of models

Model code	Simulation temperature (°C)				
	152	177	202	227	252
0	18.4 ± 0.1	18.3 ± 0.1	18.1 ± 0.1	18.0 ± 0.1	17.9 ± 0.1
1	18.5 ± 0.2	17.9 ± 0.1	17.5 ± 0.1	17.4 ± 0.2	16.4 ± 0.2
2	18.7 ± 0.2	17.8 ± 0.1	17.5 ± 0.1	17.0 ± 0.2	16.9 ± 0.2
3	18.6 ± 0.1	18.0 ± 0.1	17.4 ± 0.1	17.1 ± 0.1	17.0 ± 0.1
4	18.2 ± 0.1	18.0 ± 0.1	17.3 ± 0.1	17.2 ± 0.2	17.0 ± 0.1
5	18.2 ± 0.1	18.0 ± 0.2	17.2 ± 0.1	17.1 ± 0.2	16.9 ± 0.2
6	17.7 ± 0.2	17.7 ± 0.2	17.2 ± 0.2	16.3 ± 0.1	16.4 ± 0.2
7	17.8 ± 0.1	17.8 ± 0.2	17.0 ± 0.2	16.3 ± 0.1	16.4 ± 0.2

0 at the same temperature is 18.3 ± 0.1 $MPa^{1/2}$. Generally speaking, δ decreases with increasing temperature as well as with branch content. This is reasonable because due to Brownian motion, increasing either temperature (thermal expansion) or the number of branches enlarges the average separation of molecules and chain segments so that it lowers the cohesive energy densities.

When the δ values are used to calculate χ and the latter is plotted against temperature (Fig. 1), it is observed that when branch content is low (<25), there is only a very weak temperature dependence for χ within the ensemble fluctuations. However, when the branch content is high (above 30 branches/1000 long chain carbons), the χ vs. temperature curve goes through a maximum ($\chi > 0.025$) suggesting immiscibility at around 230 °C as shown in Fig. 1. Note that none of these curves show the inverse temperature dependence predicted by the original Flory–Huggins lattice theory. This is somewhat expected because all χ values were calculated using the computed δ values which exhibit complex T-dependence. In fact, examination of Eq. (4) reveals that χ can have temperature dependence that can be very complicated in principle. Nonetheless, data from other researchers based on PVT measurements and SANS for the 'same blend' has showed a $1/T$ temperature dependence of χ up to ~170 °C [22,23]. Such difference may be attributed to the fact that the LDPE models we used in the present work have higher concentrations of long chain branches and the associated chain ends per unit volume of the material than those of the real material. However, when Eq. (4) is used to determine χ, especially for blends containing materials having rather close δ, one basically attempts to determine very small differences between two large values. As a result, the precision of the resultant χ has to be low and the associated uncertainties are inevitably large, as illustrated in the present work. This means that even though the use of Eq. (4) is theoretically sound and

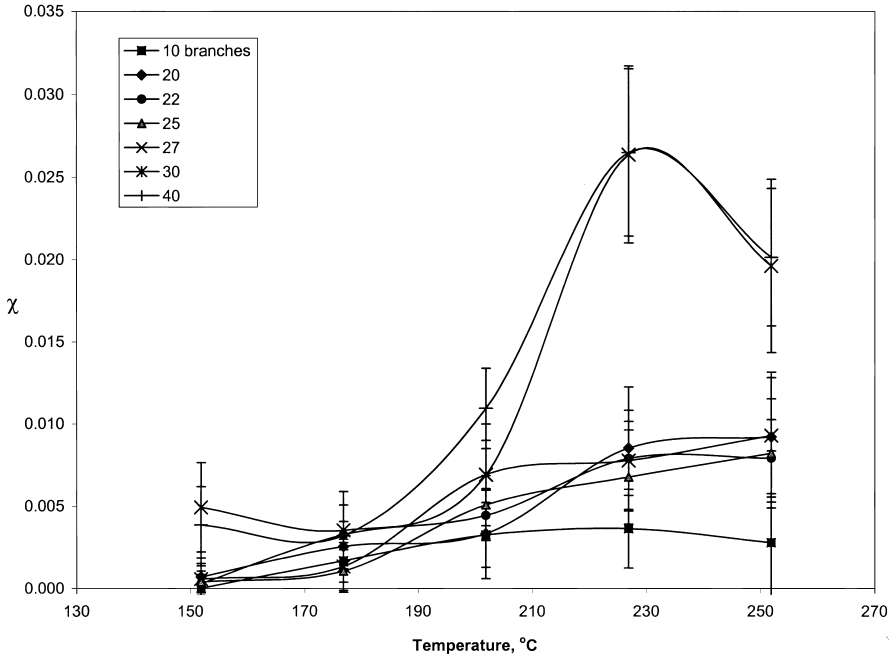

Fig. 1. χ vs. temperature for the HDPE/LDPE blends with different branch contents of LDPE.

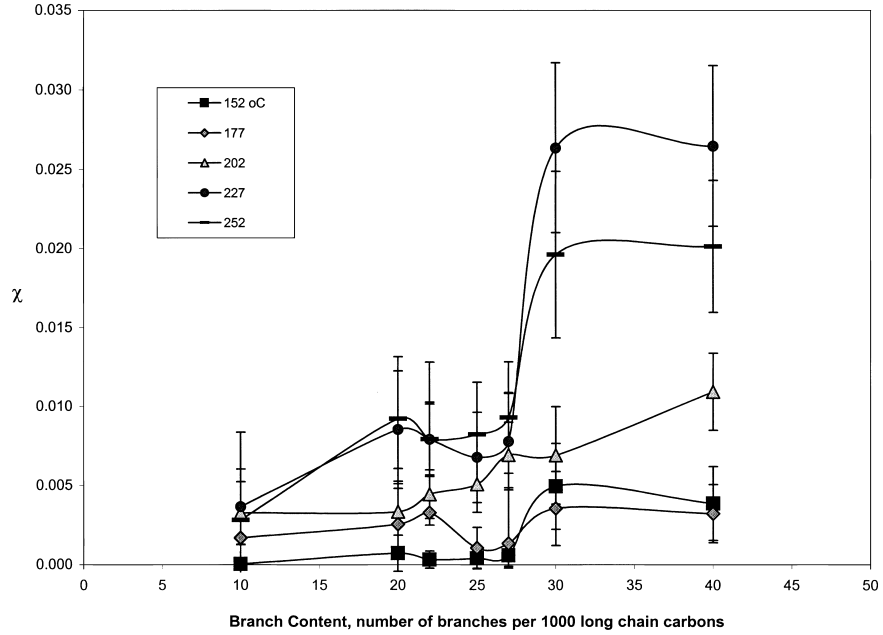

Fig. 2. χ vs. branch content for HDPE/LDPE blends at elevated temperatures.

acceptable, for binary blends containing components with nearly identical δ values, the trends of χ obtained may not be reliable. Obviously, this drawback for χ applies not only to the MD approach but also to the approaches in which the use of Eq. (4) (i.e. δ values) is required (e.g. PVT measurements). In fact, all experimental and/or computational determination of δ generally carry uncertainties in the range of ± 0.1–$0.2\ \mathrm{MPa}^{1/2}$. Therefore, it is rather difficult to judge whether which approach (e.g. MD simulation or PVT measurements) would give a more reliable temperature dependence of χ. Although temperature dependence of χ obtained from PVT measurements is in general in good agreement with those from SANS, this does not necessarily mean that such trends are more reliable than the one presented here because those trends are identified within the uncertainties of the techniques. It is worth noting that most SANS results for χ carry uncertainties in the range of 0.7×10^{-4}–1.5×10^{-4}. Since the measured χ values for polyethylene blends with small differences in branch contents (<30) from SANS are usually less than 6×10^{-4} and the variation of χ due to temperature is also rather small (on the same order of magnitude of the above-mentioned uncertainties), the temperature dependence of χ identified in this way is questionable.

Regardless of the detailed T-dependence of χ, the present results show that when the branch content of LDPE is low, χ values for the blends are rather small, near zero, the critical value of the interaction parameter for miscibility, χ_C. But when the LDPE model has a large number of branches, χ values become relatively large (i.e. far away from χ_C). The latter case implies immiscibility. In fact, when the computed χ is plotted against the branch content (Fig. 2), a step change, within the uncertainties, can be identified for the computed χ at branch values between 20 and 30 branches per 1000 long chain carbons at all temperatures, with the step more pronounced at higher temperatures. This means that when branch content of LDPE is higher than 30, blends composed of HDPE and LDPE will have a tendency to phase-separate, especially at very high temperatures ($T \geq 230\ ^\circ\mathrm{C}$). Examination of the raw data shows that the cause for such phase separation is similar to that of the HDPE/LLDPE systems reported in Ref. [6] and it is also attributed to the difference in the patterns of local packing of the two types of polyethylenes that affects the entropic part of the computed χ [6]. The cut-off value calculated above (30 branches/1000 long chain carbons) is in good agreement with the findings based upon melting point depression measurements in which Martínez-Salazar et al. found that the cut-off value should be in the range from 20 to 30 for HDPE and LDPE having rather different number molecular weight averages [24,25]. Compared with the previous molecular modeling studies [6] on the HDPE/butane-based LLDPE blends, for which the cut-off value of the LLDPE branch content was found to be around 40 branches per 1000 backbone carbons, the present cut-off value is significantly lower. Since the major topographical difference between the LDPE and LLDPE models is the long chain branches, it is suggested that long chain branching plays an important role in controlling the melt phase behavior of polyethylene blends.

4. Conclusion

Hildebrand solubility parameters of models of HDPE and LDPE with different branch contents were computed using MD simulation. The resultant values are in good agreement

with those obtained from PVT measurements. The melt miscibility of LDPE/HDPE blends was then determined by calculating their corresponding Flory–Huggins interaction parameters based upon the computed solubility parameters. Phase separation in LDPE/HDPE blends in the melt was predicted for high branch contents at high temperatures in our simulations. The cut-off value for the segregation was found to be around 30 branches per 1000 long chain carbons. The results imply that the long branches may significantly influence the miscibility of polyethylene blends. These results indicate that, $\Delta\delta$, computed by using the Dreiding force field, can be applied to capture the trend of the phase behavior of polyethylene blends. The present work shows, once again, computational success for the prediction of the melt miscibility behavior of polyethylene blends involving complex branched molecules.

Acknowledgements

We wish to thank NOVA Chemical Corporation and Natural Science and Engineering Research Council of Canada for the financial support to carry out the research. We would also like to thank Drs Charles Russell, Kam Ho and Shiv Goyal of NOVA Research and Technology Centre for valuable discussions.

References

[1] Hill MJ, Barham PJ, van Ruiten J. Polymer 1993;34(14):2975.
[2] Barham PJ, Hill MJ, Goldbeck-Wood G, van Ruiten J. Polymer 1993;34(14):2981.
[3] Hill MJ, Barham PJ. Polymer 1994;34(9):1802.
[4] Alamo RG, Graessley WW, Krishnamoorti R, Lohse DJ, Londono JD, Mandelkern L, Stehling FC, Wignall GD. Macromolecules 1997;30:561.
[5] Morgan RL, Hill MJ, Barham PJ. Polymer 1999;40:337.
[6] Choi P. Polymer 2000;41:8741.
[7] Schipp C, Hill MJ, Barham PJ, Cloke VM, Higgins JS, Oiarzabal L. Polymer 1996;37(12):2291.
[8] Barham PJ, Hill MJ, Keller A, Rosney CCA. J Mater Sci Lett 1988;7:1271.
[9] Hill MJ, Barham PJ, Keller A, Rosney CCA. Polymer 1991;32(8):1384.
[10] Hill MJ, Barham PJ, Keller A. Polymer 1992;33(12):2530.
[11] Hill MJ, Barham PJ. Polymer 1992;33(19):4099.
[12] Hill MJ, Barham PJ. Polymer 1994;35(9):1991.
[13] Alamo RG, Londono JD, Mandelkern L, Stehling FC, Wignall GD. Macromolecules 1994;27:411.
[14] Agamalian M, Alamo RG, Kim MH, Londono JD, Mandelkern L, Wignall GD. Macromolecules 1999;32:3093.
[15] Hill MJ, Puig CC. J Appl Polym Sci 1997;65:1921.
[16] Kavassalis TA, Choi P, Rudin A. In: Gubbins KE, Quirke N, editors. Molecular simulation and industrial applications—methods, examples and prospects. Amsterdam: Gordon and Breach, 1996.
[17] Allen MP, Tildelsley DJ. Computer simulation of liquids. Oxford: Oxford University Press, 1987.
[18] Rudin A, Chee KK, Shaw JH. J Polym Sci, Part C 1970;30:415.
[19] Nosé S. J Chem Phys 1984;81:511.
[20] Mayo SL, Olafson BD, Goddard WA. J Phys Chem 1990;94:8897.
[21] Han SJ, Lohse DJ, Condo PD, Sperling LH. J Polymer Sci: Part B 1999;37:2835.
[22] Graessley WW, Krishnamoorthi R, Balsara NP, Fetters LJ, Lohse DJ, Schulz D, Sissano J. Macromolecules 1994;27:3896.
[23] Zhao L, Choi P. Polymer 2001;42:1075.
[24] Martínez-Salazar J, Sánchez Cuesta M, Plans J. Polymer 1991; 32(16):2985.
[25] Plans J, Sánchez Cuesta M, Martínez-Salazar J. Polymer 1991; 32(16):2989.